385736

WSRC-RP-89-1422, Rev. 1

Al-U FUEL FOAMING/RECRITICALITY CONSIDERATIONS FOR PRODUCTION REACTOR CORE-MELT ACCIDENTS (U)

by

A. W. Cronenberg
Engineering Sciences and Analysis
8100 Mountain Road, NE
Albuquerque, New Mexico 87110

M. L. Hyder and P. G. Ellison
Westinghouse Savannah River Company
Savannah River Site
Aiken, South Carolina 29808

A paper for presentation and publication at
The American Nuclear Society International Topical of Safety of Non-Commercial Reactors Conference
Boise, Idaho
Sept. 30-Oct.4, 1990

Al-U FUEL FOAMING/RECRITICALITY CONSIDERATIONS FOR PRODUCTION REACTOR CORE-MELT ACCIDENTS

A. W. Cronenberg
Engineering Science and Analysis
8100 Mountain Road, NE
Albuquerque, NM 87110
(505) 246-0300

M. L. Hyder and P. G. Ellison
Westinghouse Savannah River Company
Savannah River Site
Aiken, SC 29808
(803) 725-4188

ABSTRACT

Severe accident studies for the Savannah River production reactors indicate that if coherent fuel melting and relocation occur in the absence of target melting, in-vessel recriticality may be achieved. In this paper, fuel-melt/target interaction potential is assessed where fission gas-induced fuel foaming and melt attack on target material are evaluated and compared with available data. Models are developed to characterize foams for irradiated aluminum-based fuel. Predictions indicate transient foaming, the extent of which is governed by fission gas inventory, heating transient condition, and bubble coalescence behavior. The model also indicates that metallic foams are basically unstable and will collapse, which largely depends on film tenacity and melt viscosity considerations. For high-burnup fuel, extensive foaming lasting tens of seconds is predicted, allowing molten fuel to contact and cause melt ablation of concentric targets. For low-burnup fuel, contact can not be assured.

INTRODUCTION

The primary purpose of the Savannah River Site (SRS) reactors is the production of tritium for national defense. For over 30 years this mission has been conducted without serious threat to the public; nevertheless, post-Chernobyl reactor safety concerns have heightened issues with regard to severe accident consequences. To provide continued assurance that the SRS reactors can be operated without undue risk, a program has been initiated to upgrade present and future production reactors to the highest safety standards. A central part of this program involves the understanding of governing phenomena and ability to quantify the consequences of low-probability/high-consequence accidents involving core meltdown.

For severe accidents the issue of recriticality is of concern, where core-melt relocation in the presence of a water moderator may, under certain conditions, lead to recriticality.[1] Such recriticality is possible for coherent fuel melting and relocation in the absence of target melting. Mixing of target and fuel melt, however, will ensure a non-critical configuration. It is of interest therefore to assess fuel/target interaction potential where the influence of fission-gas-induced fuel swelling/foaming behavior is a primary mechanism for fuel-melt attack of targets. In this paper, models are developed for the prediction of irradiated fuel foaming and foam stability characteristics. Calculational results are applied to SRS Mark-22 concentric fuel/target geometry (Figure 1). Predicted trends are compared with experimental observations on irradiated fuel foam characteristics. Conclusions are then stated with respect to the threshold burnup level at which foaming-to-fuel/target contact and aluminum-based foam stability characteristics can be assured .

M9005018

Figure 1. Illustration of Mark-22 Fuel/Target Assembly

FOAM CHARACTERIZATION

Simply stated, a foam is an agglomeration of gas bubbles separated from each other by a network of thin liquid films. Bubble morphology characteristics largely govern the extent of foaming, while the tenacity of the film network controls foam stability. For irradiated fuel, the foaming potential largely depends on changes in bubble morphology characteristics from numerous micro-bubbles to fewer but larger macro-bubbles, while foam stability is governed by the persistence of the liquid films separating the gas phase from the melt.

Figure 2 illustrates the sequence of events involved in spontaneously induced foaming for irradiated nuclear fuel.[2] Initially, fission gas is imbedded in the fuel matrix as individual atoms, followed by nucleation of micro-bubbles within the fuel matrix. Upon fuel melting, enhanced bubble coalescence, expansion, and attendant fuel swelling occur. If coalescence is rapid, the foamed state can be reached. If bubble coalescence is slow, bubble escape at the free surface may prevent the highly voided condition necessary for true foaming. Thus, foaming is largely a race between bubble nucleation, growth, and coalescence versus gas escape from the melt.

Figure 2. Sequence of Events Associated With Irradiated Fuel Foam Formation and Destruction

Once formed, foams tend to collapse as a result of film destruction. Drainage of the intervening film between two adjacent bubbles will lead to foam collapse. Quantitative models for the assessment of foam formation and stability characteristics as presented in this paper are applied to SRS conditions.

Foam Inducement

The extent of foaming for irradiated fuel upon melting can be calculated as the sum of several contributions associated with the expansion of the fuel upon melting and changes in bubble morphology within the melt; i.e.:

$$F_{total} = F_{matrix} + F_{st} + F_{bc} + F_{th} \quad (1)$$

where F_{matrix} is the expansion of the fuel cell upon melting, F_{st} is the change in bubble volume resulting from the lowered surface tension upon solid-to-liquid phase transformation, F_{bc} is the volumetric expansion resulting from bubble coalescence, F_{th} is thermally induced bubble growth, and the fractional extent of volumetric swelling (F) for an individual mechanism can be expressed as:

$$F = (V_{final} - V_{initial})/V_{initial} \quad (2)$$

where V is the volume of a unit fuel cell (i.e., 1 cm^3). Fuel matrix expansion upon melting can be estimated as:

$$F_{matrix} = (\rho_s/\rho_m)^{-1} \quad (3)$$

where ρ_s and ρ_m are the densities of the solid and melt respectively. Noting that the aluminum density at room temperature is about 2.7 g/cm^3 versus 2.38 g/cm^3 at melting, the volumetric swelling resulting from density changes is about 13 percent.[a]

The influence of a reduction in surface tension (σ) on the volume occupied by fission gas bubbles in the melt versus solid can be assessed from the the following equilibrium force balance.

$$(2\sigma_s + PR_s) R_s^2 = (2\sigma m + PR_m)R_m^2 \quad (4)$$

where P is ambient pressure, and σ_s and σ_m are the solid and melt surface tensions, respectively.

Noting that the bubble concentration (N, bubbles/cc-fuel) can be estimated as:

$$N = N_g/N_{gb} \quad (5)$$

---

[a] F_{matrix} is dependent on UAl_x alloying composition, where little expansion is expected upon melting for high uranium content resulting from reduced ρ_s with increased uranium.

where N_g is the number of gas atoms per unit volume, N_{gb} is the number of gas atoms per bubble of radius R and can be estimated from the following equation of state for microbubbles.[3]

$$N_{gb} = \frac{V_b}{[A + BR]} \tag{6}$$

where V_b equals bubble volume, A equals 85 E-24 cm^3, B equals $kT/2\sigma$, k equals Boltzmann's constant, and T equals temperature.

The fractional swelling caused by changes in surface tension can thus be evaluated from solution of equation (4) in conjunction with equations (5 and 6), yielding:

$$F_{st} = \frac{N(4\pi/3)[R_m^3 - R_s^3]}{1 + N(4\pi/3)R_s^3} \tag{7}$$

As shown in Table 1, surface tension effects on melting are quite limited and estimated to contribute a maximum volumetric swelling of about fourteen percent for large bubbles (200,000 A°) associated with high-burnup conditions (50 atom-percent). At lower burnups and smaller bubble radii, the effect is much lower. Because a three-fold volumetric swelling is required to ensure good fuel/target contact for Savannah River Mark-22 assemblies, changes in fuel density and surface tension upon melting are not sufficient to account for fuel/target contact. The primary mechanisms for foam inducement, therefore, relate to changes in bubble morphology caused by enhanced bubble coalescence in the melt and thermally induced bubble expansion.

Upon fuel melting, an increase in bubble mobility occurs, inducing coalescence of numerous microbubbles into fewer but larger bubbles with attendant fuel swelling. Coalescence will result in continued bubble growth and fuel swelling until large bubbles try to escape from the melt by bouyancy-driven forces or other bubble escape mechanisms. Thus, the extent of foaming can be viewed as largely a race between bubble coalescence versus escape. Two approaches were employed to define the maximum extent of bubble coalescence. The first is based on determination of the critical bubble radius (R_c) at which bouyancy-induced bubble escape just matches that of bubble migration/coalescence by volume diffusion; i.e.,

$$R_c = [(9/8\pi)(1/\rho g)(Q/r_a)(\Delta T/T)]^{0.5} \tag{8}$$

where ΔT equals temperature gradient, T equals temperature, Q equals activation energy for volume diffusion, r_a equals atomic radius, ρ equals melt density, and g equals gravitation constant.

Equation (8) yields coalescence to a limit of about 20,000 A° based on equilibrium between escape and coalescence; while at high-transient heating conditions, a nonequilibrium condition exists so that larger bubble radii can be expected. Thus, equation (8) yields a lower limit of coalescence.

Table 1. Swelling Caused by Surface Tension Effects

Parameter Values

σ_s = 1000 dy/cm

σ_m = 914 dy/cm

P = 1 atm (1.0E+6 dy/cm^2)

N_g = 2.0 E+20 gas-atoms/cc-fuel (at 50-percent atom burnup)

Calculation

$R_{b,s}$, A° (cm)	$R_{b,m}$, A°	N, (bubbles/cc)	Fractional Swelling (F_{st})
10 (1.0E-7)	10.46	4.44 E+18	0.003
1000 (1.0E-5)	1045	4.01 E+13	0.020
10,000 (1.0E-4)	10,440	3.64 E+11	0.081
20,000 (2.0E-4)	20,830	9.07 E+10	0.098
200,000 (2.0E-3)	209,000	9.01 E+8	0.137

For high nonequilibrium conditions, bubble coalescence is based on the condition that the gas retained in melt coalesces into large bubbles that are essentially free of their surface tension restraint; i.e.:

$$Rc = 2(\sigma)/P \simeq 200{,}000\ A° \quad . \tag{9}$$

Knowing the bubble size and density characteristics for both the initial (uncoalesced) and final (coalesced) states, the fractional volume expansion from bubble coalescence (F_{bc}) can be assessed from the following equation.

$$F_{bc} = \frac{(4\pi/3)[N_2R_2^3 - N_1R_1^3]}{1 + N_1(4\pi R_1^3/3)} \quad \text{and} \quad R_2 = R_c \tag{10}$$

where the subscripts 1 and 2 refer to the initial (uncoalesced) and final (coalesced) states, respectively.

A similar expression for fractional swelling (F_{th}) resulting from an increase in fuel temperature can be defined where, in this case, the bubble density (N) remains constant and ideal gas behavior is assumed; i.e.:

$$F_{th} = \frac{N(4\pi/3)(R_2^3 - R_c^3)}{1 + N(4\pi R_c^3/3)} \quad \text{and} \quad R_2 = [(T_2/T_1)R_c^2]^{0.5} \tag{11}$$

where R_c is the critical bubble radius for coalescence in the melt before thermally induced bubble expansion.

Calculation results as a function of fuel temperature (1000 and 1500 K), burnup (50, 5, and 1 atom-percent), and extent of bubble coalescence (R_c = 20,000 - 200,000 A°) are summarized in Table 2 where R_1 equals 10 A° and T_1 equals 500 K, which is characteristic of normal Mark-22 operational conditions. Results indicate that at elevated burnup (50 atom-percent) and temperature (1000 to 1500 K), a large scale increase in volumetric swelling can be expected so that Mark-22 fuel/target contact is assured (i.e., a three-fold increase in fuel melt volume is required for fuel/target contact). However, at reduced burnups and associated limited gas inventory conditions, the predicted extent of fuel swelling/foaming is insufficient to cause fuel/target contact. It is also interesting that temperature gradient effects are of importance, where enhanced bubble mobility/coalescence is predicted at increased gradients as demonstrated in equation (8) where increased ΔT yields larger R_c. The foaming potential would thus be enhanced for increased transient heating conditions.

Foam Stability

Although large-scale foaming is predicted for high burnup, the question arises as to the stability characteristics of such metallic foams and whether sufficient time exists for target melting. The characteristic time for target melting can be approximated from the following equation for the thermal relaxation period.

$$t_{t,m} \simeq X^2/(\alpha a^2) \tag{12}$$

where α equals thermal diffusivity, X equals target thickness, and the solidification constant (a) can be assessed from equation (13).

$$C_p(T_{mp} - T)/L \simeq a \exp(a^2) \tag{13}$$

where C_p equals specific heat, T_{mp} equals melting point, T equals initial target temperature, and L equals the latent heat of fusion.

Table 3 indicates that for aluminum-based targets and Mark-22 geometry, a thermal relaxation time of 1.3 seconds (s) is estimated. Thus, fuel foam must be stable for several seconds in order to initiate target melting.

Table 2. Summary of Predicted Foaming Behavior of Irradiated U-Al Fuel

Initial Conditions: $R_1 = 10$ A° $T_1 = 500$ K

Burnup (percent)	Temperature T_2 (K)	Fractional Bubble Coalescence (F_{bc} at R_c)	Fractional Bubble Thermal Expansion (F_{th})	Total Volumetric Swelling ($F_t = F_{bc} + F_{th}$)
50	1000	2.97 (20,000 A°)	1.37	4.34
	1500	2.97 (20,000 A°)	3.16	6.13
	1000	29.6 (200,000 A°)	1.74	31.34
	1500	29.6 (200,000 A°)	4.06	33.66
5	1000	0.30 (20,000 A°)	0.43	0.73
	1500	0.30 (20,000 A°)	0.98	1.28
	1000	3.00 (200,000 A°)	1.37	4.37
	1500	3.00 (200,000 A°)	3.15	6.15
1	1000	0.06 (20,000 A°)	0.10	0.16
	1500	0.06 (20,000 A°)	0.24	0.30
	1000	0.60 (200,000 A°)	0.69	1.29
	1500	0.60 (200,000 A°)	1.58	2.18

Table 3. Estimated Target Thermal Relation Time

Parameter Values (Al-melt)

$C_p = 0.26$ cal/g-K
$T_{mp} = 933$ K
$T = 600$ K
$L = 95$ cal/g
$k = 0.25$ cal/s-cm-K
$\rho = 2.38$ g/cm^3
$\alpha = k/\rho C_p = 0.4$ cm^2/s
$a = 0.62$

Calculation

$C_p(T_{mp} - T)/L = 0.91$

X(Mark-22 inner target) = 2.019 cm - 1.57 cm = 0.449 cm

$t_{t,m} \simeq X^2/(\alpha a^2) \simeq 1.3$ seconds

To evaluate foam stability characteristics, the time scale for thinning/destruction of the film lamellae between two large coalesced bubbles is assessed for the geometry illustrated in Figure 3, where the velocity profile is based on the solution of the Navier-Stokes equation for film flow as developed by Lee and Hodgson.[4]

$$V(r,z) = \frac{\Delta P}{\mu}\left[\left(\frac{h^2}{2}\right) - z^2\right](r/R_f^2) \tag{14}$$

where h equals film thickness, ΔP equals pressure differential, and R_f equals radius of film disk. Application of mass continuity for the rate of film thinning in the Z and r directions yields the following relationship.[5]

$$-\frac{dh}{dt} = \frac{h^3 \Delta P}{3\mu R_f^2} \tag{15}$$

This relationship, upon integration from the original film thickness (h_o) to the critical thickness (h_c) at which film destruction occurs, yields the time for film destruction by thinning.[5]

$$\int_{h_o}^{h_c} -h^{-3}\, dh = \frac{\Delta P}{3\,\mu\, R_f^2}\int_{o}^{t_t} dt \tag{16}$$

$$t_t = \frac{3\,\mu\, R_f^2}{2\Delta p}\left(\frac{1}{h_c^2} - \frac{1}{h_o^2}\right) \tag{17}$$

Because $h_o >> h_c$, the film destruction time can be approximated as:

$$t_t \simeq \frac{3\,\mu\, R_f^2}{2\,\Delta P\, h_c^2} \tag{18}$$

Figure 3. Film Thinning Model Between Two Large Coalesced Bubbles at Onset of Foam Destruction

It is interesting that the film thinning time is essentially independent of the original film thickness, but rather depends on the length of the film ligament (Rf) and the critical film thickness (hc) at which rupture occurs. For practical purposes, Rf ≃ R (bubble radius), while the pressure differential on vertical film lamellae can be approximated as $\Delta P \simeq R\rho g$; thus:

$$t_t \simeq \frac{3 \mu R}{4 \rho g h_c^2} \qquad (19)$$

where ρ is the melt density and g is the gravitation constant (980 cm/s^2).

Several criteria[6] have been suggested for estimation of h_c. DeVries[7] proposed that rupture of film lamellae occur by wave instabilities at thickness of about 100 A°. In a nuclear radiation environment, puncturing of films by fission-fragment ionization (stopping length of 1000 A°)[8] may be a more appropriate criteria for h_c.

Table 4 presents predicted film thinning times at various h_c and final coalesced bubble radii. As indicated, the film drainage time (and thus foam stability) is largely controlled by the critical thickness (h_c) at which film rupture occurs. If film thinning down to 100 A° occurs, then drainage times on the order of tens of minutes are estimated. In a radiation field (h_c = 1000 A°), a much shorter time is estimated, that is on the order of tens of seconds.

Table 4. Estimated Film Destruction Times

Parameter Values, Al-melt

μ = 0.015 g/s-cm
ρ = 2.38 g/cm^3
g = 980 cm/s^2
$3\mu/4\rho g$ = 4.823 E-6 cm-s

Bubble Radius, R (A°)	Critical Film Thickness, h_c (A°)	Film Thinning Time, t_t (s)
20,000	100	965 (≃ 16 min)
	1000	9.65
200,000	100	96.50 (≃ 160 min)
	1000	96.5

DISCUSSION AND COMPARISON WITH EXPERIMENTAL OBSERVATIONS

The results of the foregoing analysis indicate some of the essential features of foam formation and stability for irradiated aluminum-based alloy fuel. Of particular note is the overriding dependance of the foaming potential on fission gas inventory and the extent of bubble coalescence as revealed by equation (10). Fuel at low fission gas inventory and corresponding low bubble concentrations (N) exhibit limited foaming potential. The extent of volumetric foaming is also largely determined by bubble morphology conditions; that is, the amount of bubble coalescence (R_c) and thermally induced bubble expansion. The more pronounced the extent of bubble coalescence, the greater the volumetric swelling. Thus, at a particular burnup condition, larger but fewer bubbles will lead to greater foaming than numerous but smaller bubbles. It is from this perspective that foaming can be viewed largely as a race between coalescence and fission gas bubble escape from the melt.

In the analysis presented, the limit of bubble coalescence (i.e., critical bubble radius, R_c) was defined using two criteria. The first is based on the condition of equilibrium between bouyancy-induced bubble escape from the melt versus coalescence by a volume diffusion mechanism. Such a coalescence limit does not account for other contributions to bubble mobility (e.g., evaporation/condensation, stress-induced bubble mobility, sweeping of gas atoms by bubbles) or the various factors that contribute to gas escape from the melt (e.g., interlinking of bubbles, melt breakup). Thus, predicted values of the coalescence limit (R_c) are approximate and represent a lower limit of coalescence. The second criterion is based on the condition that bubble coalescence occurs to a maximum limit of 200,000 A°, at which, bubbles are free of their surface tension constraint. At large coalesced bubble radii (200,000 A°) and elevated burnup conditions (50 atom-percent), a 30-fold increase in volumetric swelling is predicted (Table 2). The effect of burnup at large bubble radii (200,000 A°) is also illustrated in Table 2, indicating that, at about two-percent burnup, the volumetric expansion requirements for Mark-22 fuel/target contact are satisfied (i.e., three-fold volumetric expansion).

Although extensive foaming is predicted for high-burnup aluminum-based fuel, such metallic foams are unstable and collapse as a result of destruction of the thin film lamellae that constitute the film network characteristic of the foamed condition (Figures 2 and 3). The time scale for film destruction was characterized from consideration of gravity-induced film drainage where thinning to a critical film thickness (h_c) results in film destruction and onset of foam collapse. Predicted film thinning times exhibit a 2ed power dependence on h_c; thus, foam stability is considered to be largely dependent on the film thickness (h_c) at which film rupture occurs. For a radiation environment, film puncturing by ionization at $h_c \simeq 1000$ A° yields an onset time of foam collapse of tens of seconds. In a non-radiation environment, films are considered stable to 100 A°, with corresponding film thinning times on the order of tens of minutes.

Although the modeling approach outlined is approximate and considers only first order effects; nevertheless, it serves as a basis for prediction of overall trends. These trends are compared here with experimental observations. Revealing experiments are those conducted in the early 60s by Buddery and Scott [9], where fission gas release and swelling of molten uranium metal was examined. Natural uranium samples were heated out-of-pile to uranium-melting temperatures (T_{mp} = 1405 K) at fission gas densities of about 2.0 E+19 gas-atoms per cc-fuel (corresponds to about five-percent burnup for SRS fuel). Transient swelling and collapse behavior was characterized from fuel volume and density estimates, which are plotted in Figure 4 in terms of fuel-specific volume. Initial swelling is evident with subsequent collapse upon fission gas release from the melt. More than 99 percent of the Kr^{85} (measured during

Figure 4. Experimental Swelling/Foaming Behavior Noted for Previously-Irradiated Uranium Metal Fuel Brought to Melt Temperatures

testing) was lost on melting. Rapid gas release began about 10°C below the melting point and increased once melting occurred. The final configuration was a once-molten pool of almost full-density uranium covered by a low-density froth.

Based on such observation Buddery and Scott[9] concluded that, for irradiated metallic fuel, initial foaming behavior can be expected, followed by rapid froth collapse upon release of previously entrapped fission gas. The final density of the fuel can be expected to be close to that of the initial density prior to heating. They also concluded that although burnup and melt temperature had a large impact on the extent of foaming, these parameters had little effect on the rate of gas release and foam collapse. Such experimental observations are in general agreement with predicted modeling trends (i.e., initial foaming at fuel melting with subsequent foam collapse upon release of entrapped fission gases). It is interesting that the half width of the swelling/collapse peak shown in Figure 4 is on the order of 15 seconds. This experimental value compares favorably with the film destruction times ot tens of seconds predicted here, assuming film puncture at $h_c \simeq 1000$ A°.

CONCLUSIONS

Models of transient foaming and collapse behavior for irradiated metallic fuel heated to melt temperatures indicate that the foaming potential is governed by fission gas inventory conditions. Fuel at low fission gas inventory and corresponding low bubble concentrations exhibit limited foaming potential; whereas higher burnup fuel exhibits a high potential to foam. The actual extent of volumetric foaming, however, is largely determined by bubble morphology conditions, (i.e., the amount of bubble coalescence and thermally induced bubble expansion). The more pronounced the extent of bubble coalescence, the greater the volumetric swelling; thus, at a particular burnup condition, larger but fewer bubbles will lead to greater foaming than numerous but smaller bubbles. Fuel foaming can therefore be viewed largely as a race between coalescence and fission gas escape from the melt. For Mark-22 aluminum-based alloy fuel at transient heating conditions, burnups in excess of about two atom percent is predicted to result in sufficient fuel volumetric swelling to induce fuel melt/target contact.

Although extensive foaming is predicted at such burnup conditions, metallic foams are predicted to be unstable and to collapse because of destruction of the thin film lamellae that constitute the film network characteristic of the foamed state. The timing of collapse will depend on several factors, including the film thickness at which rupture occurs, melt geometry, and viscosity. Aluminum-based foams lasting tens of seconds are predicted for radiation environments resulting from film ionization at a thickness of 1000 A°, while longer foam lifetimes are predicted for nonradiation environments (tens of minutes) where films are considered stable to 100 A°.

For Mark-22 geometry, fuel foaming at greater than two-percent burnup is predicted, sufficient to induce fuel melt contact with target material and remain stable for tens of seconds, which would allow for onset of target melting. However, for low-burnup fuel, fuel/target contact can not be assured.

REFERENCES

1. J. P. MORIN, K. A. WILLIAMS, C. N. AMOS, M. T. LEONARD, and P. K. MAST, *Severe Accident Assessment Program: Preliminary Characterization of Existing Savannah River Production Reactor Severe Accident Behavior and Modeling Requirements*, DPST-88-999, SAA-10 (December 1988).

2. A. W. CRONENBERG, D. W. CROUCHER, AND P. E. MACDONALD, "Fuel Foaming and Collapse During LWR Core Meltdown Accidents", *J. Nucl. Tech.*, 312-325 (1984).

3. D. OLANDER, *Fundamental Aspects of Nuclear Reactor Fuel Elements*, ERDA Publication, 204 (1976).

4. J. C. LEE AND T. D. HODGSON, "Film Flow and Coalescence: Basic Relations, Film Shape, and Criteria for Interface Mobility," *Chemical Engineering Science*, 23 1375-1397 (1968).

5. A. W. CRONENBERG, D. W. CROUCHER, AND P.E. MACDONALD, *An Assessment of Fuel Foaming Potential During Core Meltdown Accidents, NUREG/CR-2701, EGG-2191*, (October 1982).

6. I. L. JASHNANI AND R. LEMLICH, "Foam Drainage, Surface Viscosity, and Bubble Size Bias", *Colloidal and Interfacial Science (46)*, 13-16 (1974).

7. A. J. DEVRIES, *Foam Stability*, Delft, The Netherlands, Rubber-Stichting Publishing Company (1957).

8. J. H. CHUTE, "Direct Observations of Fission Fragment Damage in Ceramic Oxides," *Journal of Nuclear Materials*, (21), 77-87 (1967).

9. H. BUDDERY AND K. T. SCOTT, "A Study of The Melting of Irradiated Uranium", *Journal of Nuclear Materials*, (5), 81-93 (1962).

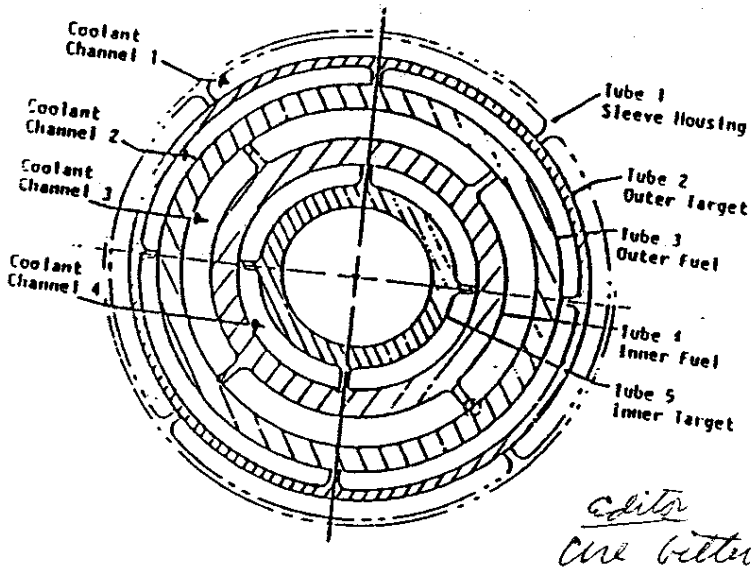

Editor
Can better SRS
picture of Mark-22 assembly,
with dimensions if allowable?

Figure 1. Illustration of Mark-22 Fuel/Target Assembly

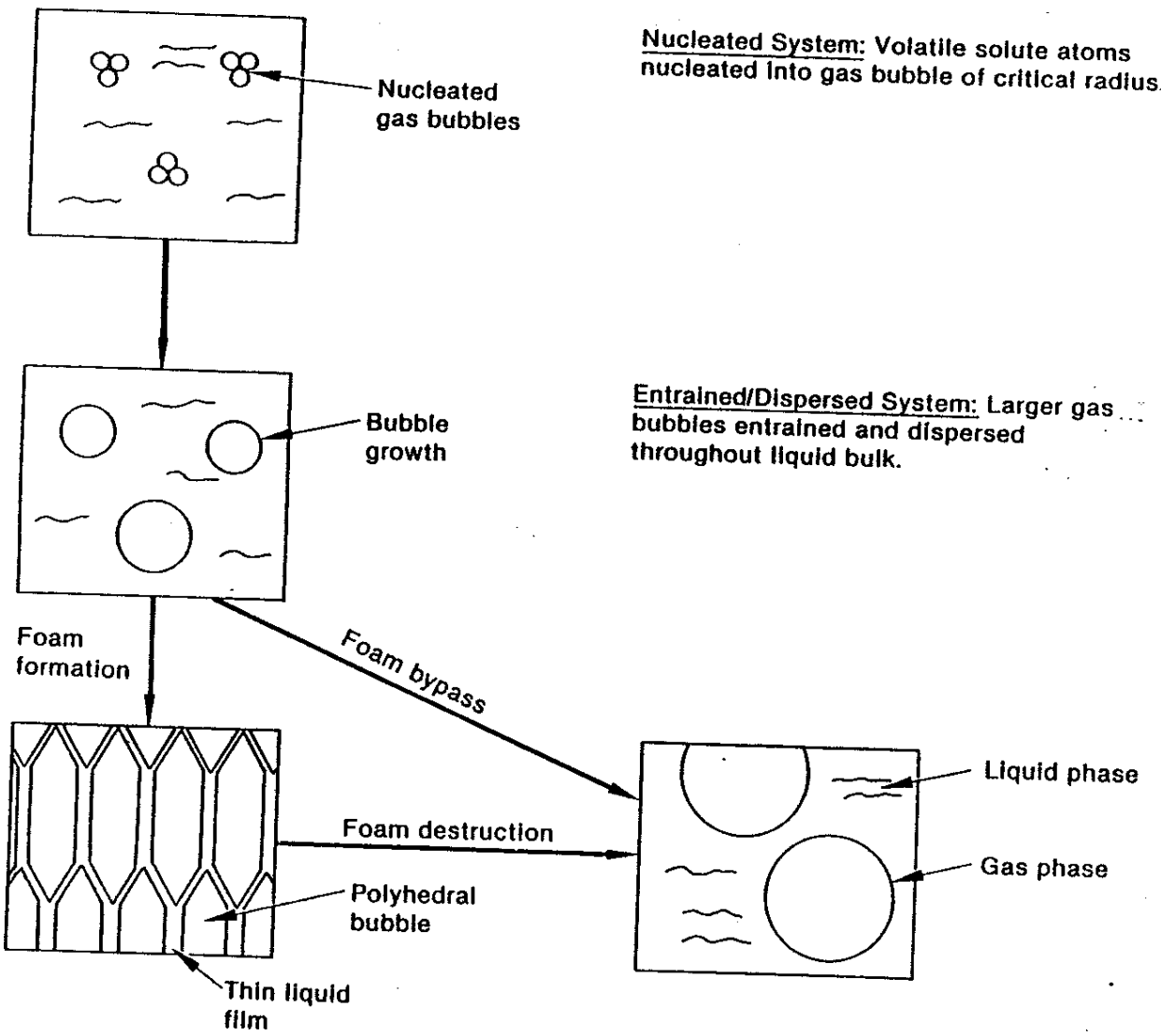

Nucleated System: Volatile solute atoms nucleated into gas bubble of critical radius.

Entrained/Dispersed System: Larger gas bubbles entrained and dispersed throughout liquid bulk.

Foams: Agglomeration of gas bubbles separated from each other by thin liquid films.

Coalesced/Separated System: Gas bubble coalescence, tending to form a separated gas/liquid system.

INEL 2 0795

Fig 3

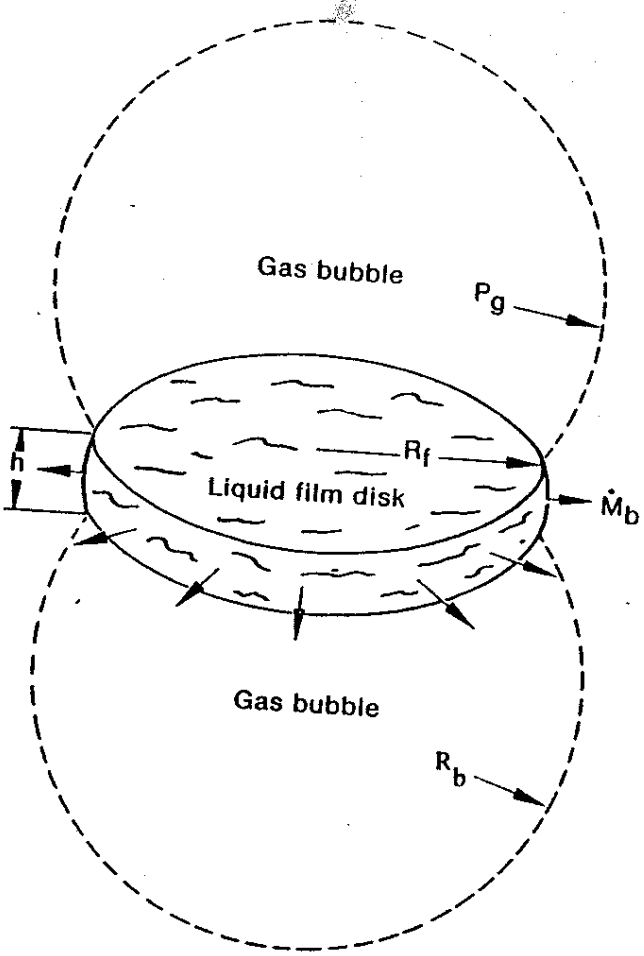

Illustration of liquid film flow due to bubble coalescence

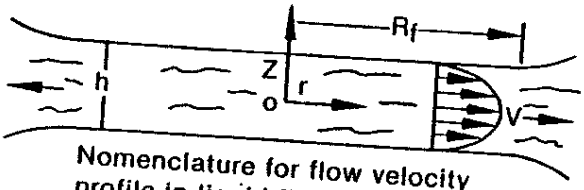

Nomenclature for flow velocity profile in liquid film disk using a rigid-wall, parallel-plate model

INEL 2 0794

Make - PMT or glossy print or one of these Figs for Fig 3 paper

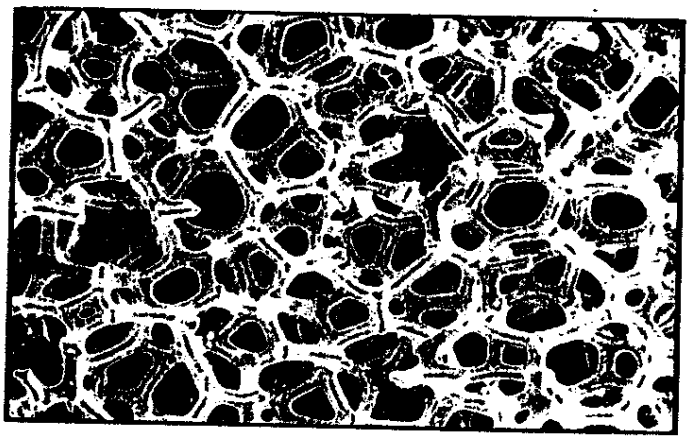

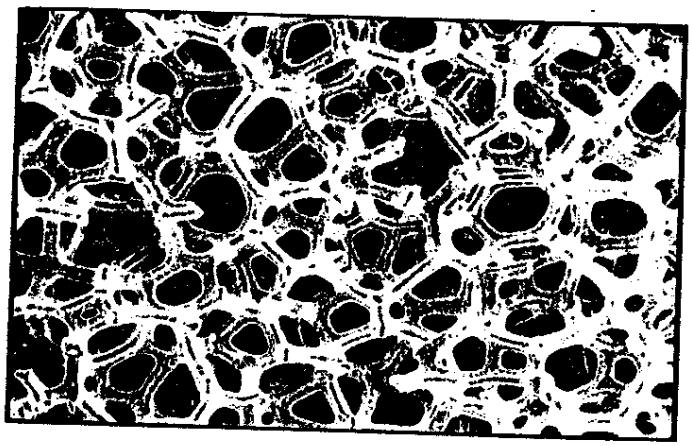

[illegible]

[illegible]